OXFORD
SOT | Society of Toxicology
www.toxsci.oxfordjournals.org

TOXICOLOGICAL SCIENCES, 142(1), 2014, 210–224

doi: 10.1093/toxsci/kfu169
Advance Access Publication Date: August 21, 2014

Incorporating Population Variability and Susceptible Subpopulations into Dosimetry for High-Throughput Toxicity Testing

Barbara A. Wetmore*,[1], Brittany Allen*, Harvey J. Clewell, III*, Timothy Parker*, John F. Wambaugh†, Lisa M. Almond‡, Mark A. Sochaski*, and Russell S. Thomas*,[2]

*The Hamner Institutes for Health Sciences, Research Triangle Park, North Carolina 27709-2137, †United States Environmental Protection Agency, Office of Research and Development, National Center for Computational Toxicology, Research Triangle Park, North Carolina 27711 and ‡Simcyp Limited (a Certara company), Blades Enterprise Centre, John Street, Sheffield S2 4SU, UK

[1]To whom correspondence should be addressed at The Hamner Institutes for Health Sciences, 6 Davis Drive, PO Box 12137, Research Triangle Park, NC 27709. Fax: (919) 558-1300. E-mail: bwetmore@thehamner.org.
[2]Present address: United States Environmental Protection Agency, Office of Research and Development, National Center for Computational Toxicology, Research Triangle Park, NC 27711.

ABSTRACT

Momentum is growing worldwide to use *in vitro* high-throughput screening (HTS) to evaluate human health effects of chemicals. However, the integration of dosimetry into HTS assays and incorporation of population variability will be essential before its application in a risk assessment context. Previously, we employed *in vitro* hepatic metabolic clearance and plasma protein binding data with *in vitro in vivo* extrapolation (IVIVE) modeling to estimate oral equivalent doses, or daily oral chemical doses required to achieve steady-state blood concentrations (C_{ss}) equivalent to media concentrations having a defined effect in an *in vitro* HTS assay. In this study, hepatic clearance rates of selected ToxCast chemicals were measured *in vitro* for 13 cytochrome P450 and five uridine 5′-diphospho-glucuronysyltransferase isozymes using recombinantly expressed enzymes. The isozyme-specific clearance rates were then incorporated into an IVIVE model that captures known differences in isozyme expression across several life stages and ethnic populations. Comparison of the median C_{ss} for a healthy population against the median or the upper 95th percentile for more sensitive populations revealed differences of 1.3- to 4.3-fold or 3.1- to 13.1-fold, respectively. Such values may be used to derive chemical-specific human toxicokinetic adjustment factors. The IVIVE model was also used to estimate subpopulation-specific oral equivalent doses that were directly compared with subpopulation-specific exposure estimates. This study successfully combines isozyme and physiologic differences to quantitate subpopulation pharmacokinetic variability. Incorporation of these values with dosimetry and *in vitro* bioactivities provides a viable approach that could be employed within a high-throughput risk assessment framework.

Key words: *In vitro in vivo* extrapolation; population variability; toxicokinetics; reaction phenotyping; dosimetry; risk assessment

Over the past five years, high-throughput *in vitro* screening (HTS) has been advocated as the future of toxicity testing (Andersen and Krewski, 2009; Collins *et al.*, 2008; NRC, 2007). The ability to screen thousands of chemicals across hundreds of molecular targets and pathways provides an efficient, economical, and humane alternative to the current use of high-dose animal-based

studies. Although these attributes make HTS desirable within a toxicity testing framework, several key considerations need to be addressed before it can be realistically considered within the context of risk assessment. First, the chemical concentration in a well that elicits *in vitro* biological activity may be different from the blood or tissue concentration required to elicit a comparable *in vivo* response due to bioavailability, clearance, and other pharmacokinetic (PK) considerations (Blaauboer, 2010). Second, the HTS data—in particular the concentrations at which perturbations may occur—need to be viewed in the context of anticipated exposure levels to gauge the relevance of a biological effect occurring given a proposed exposure scenario (Cohen Hubal *et al.*, 2010; NRC, 2007). Third, HTS data provide little consideration of variability in responses due to PK or pharmacodynamic differences among subpopulations.

To address the first two issues, we previously measured *in vitro* hepatic clearance and plasma protein binding for 239 ToxCast chemicals and performed *in vitro in vivo* extrapolation (IVIVE) to determine steady-state blood concentrations (C_{ss}) that would be predicted given repeated, daily exposure (Rotroff *et al.*, 2010b; Wetmore *et al.*, 2012). These values were then used in conjunction with ToxCast HTS data (Houck *et al.*, 2009; Huang *et al.*, 2011; Judson *et al.*, 2010; Knight *et al.*, 2009; Knudsen *et al.*, 2011; Martin *et al.*, 2010; Rotroff *et al.*, 2010a) to estimate the daily oral dose, known as the oral equivalent dose, necessary to produce steady-state *in vivo* blood concentrations equivalent to the AC_{50} (concentration at 50% of maximum activity) or LEC (lowest effective concentration) values in the *in vitro* assays. These values were then compared with human exposure estimates derived from US Environmental Protection Agency (EPA) pesticide regulatory documents to assess whether anticipated exposures fell at levels that could potentially elicit biological activity measured in the *in vitro* assays. Hepatic clearance was measured using primary hepatocytes derived from a pool of healthy male and female adults from 20–50 years of age. As a result, the oral equivalent dose values were estimated for a population of general, healthy adults. Further, although hepatocytes are routinely used to estimate hepatic intrinsic clearance, this system provides no insight into the relative contribution of individual phase I and II metabolic isozymes to chemical clearance.

Risks associated with xenobiotic exposure can vary for humans from different life stages or ethnicities for a variety of reasons. Differing exposure scenarios brought on by dietary, behavioral or physiological differences can affect the extent of exposure (EPA, 2011; NRC, 1993). Children, for instance, have a greater inhalation and food ingestion rate per unit body weight and are more likely to come in contact with contaminants present in soil and house dust than other subgroups. Xenobiotic clearance rates in humans are also known to vary throughout life, with significantly different rates noted in gestational and neonatal life stages compared with juvenile, adult, and geriatric populations (Ginsberg *et al.*, 2005, 2002; Schmucker, 2005; Tanaka, 1998). Differences in other PK factors such as protein binding, volume of distribution, and hepatic blood flow all contribute to this variability (Besunder *et al.*, 1988a,b; Ginsberg *et al.*, 2005, 2002; Kearns *et al.*, 2003; Schmucker, 2005). Consequently, the reliance on a generalized adult population as the basis of comparison between the oral equivalent dose values for the *in vitro* assays and human exposure estimates could significantly underestimate the risk to other populations.

With the majority of drugs and xenobiotics metabolized by the cytochrome P450 (CYP)-dependent monooxygenase and the uridine 5′-diphospho-glucuronosyltransferase (UGT) systems, any differences in the expression of these enzymes can significantly impact clearance rates. Life stage-based differences in the abundances of CYPs 1A2, 2C8, 2C9, 2C18, 2C19, 2D6, 2E1, 3A4, and UGTs 1A1, 1A4, 1A6, 1A9, and 2B7 have been documented and extensively characterized from fetal and pediatric life stages to the adult (Cresteil, 1998; Hines, 2007; Johnson *et al.*, 2006; Kearns *et al.*, 2003; Leakey *et al.*, 1987; Miyagi and Collier, 2007; Salem *et al.*, 2013; Yokoi, 2009). Genetic polymorphisms of CYPs 2B6, 2C9, 2C19, and 2D6 have also been well characterized, resulting in differing drug metabolizing capabilities for up to 20% of the Asian population for CYP 2C19 substrates and 10% of the Caucasian population for CYP2D6 substrates (Hiratsuka, 2012; McGraw and Waller, 2012). Incorporation of these enzyme differences in the measurement of xenobiotic clearance rates would provide key information in determining the range and extent of inter-individual PK variability.

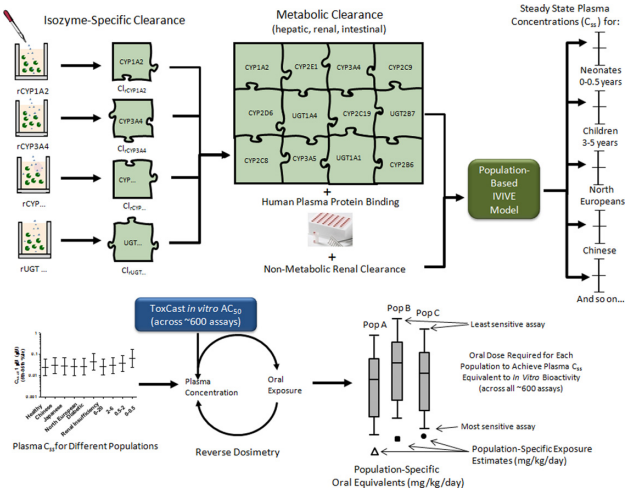

FIG. 1. Schematic representation of approach to incorporate population-specific dosimetry with high-throughput *in vitro* screening data. Isozyme-specific clearance rates for each chemical were measured across 18 recombinantly expressed cytochrome P450s and UGTs. Using a population-based *in vitro in vivo* extrapolation model (IVIVE), steady state plasma concentrations (C_{ss}) were predicted by incorporating experimentally measured plasma protein binding and isozyme-specific clearance data with population-specific physiology and isozyme ontogenies scaled to capture known abundances across different life stages and ethnic populations. Population-specific C_{ss} values were predicted; in addition, Monte Carlo simulations captured variability within each population, with median, lower, and upper 95th percentile values obtained as output. Using reverse dosimetry, population-specific plasma C_{ss} were incorporated with chemical *in vitro* bioactivity concentrations as measured in ToxCast to estimate population-specific oral equivalents. These values can then be compared against population-specific exposure estimates.

In this study, we outline an approach to link *in vitro* HTS results with subpopulation-specific dosimetry and exposure estimates. For subpopulation dosimetry, *in vitro* intrinsic clearance of a subset of nine ToxCast chemicals was determined across a panel of recombinant CYP (13) and UGT (5) isozymes and used in conjunction with population databases describing the genetic, ethnic, and life-stage (ontogeny)-related differences in enzyme abundance and physiology (Fig. 1). This approach allowed the estimation of oral equivalent dose values for each of the previously published ToxCast assays across a range of life stages and ethnic populations. The oral equivalent doses for each chemical-assay combination were compared with the corresponding exposure estimates for each population. The approach also provides the ability to estimate chemical-specific human toxicokinetic adjustment factors (HK_{AF}) for use in risk assessment (IPCS, 2005) (Lipscomb *et al.*, 2004).

MATERIALS AND METHODS

Chemical selection. With the goal of this effort to inform safety assessments and/or priority setting, selected chemicals needed to meet certain criteria to evaluate the approach. All nine of the chemicals were screened for bioactivity across over 700 HTS assays and a range of technologies as a part of the US EPA's ToxCast program (Judson *et al.*, 2010). Seven of the nine were selected due to the availability of regulatory exposure estimates to allow derivation of a population-specific margin of exposure. Availability of hepatocyte clearance data in previous work (Wetmore *et al.*, 2012) enabled the inclusion of chemicals that spanned a range of clearance rates (low, medium, high). In addition, three of the chemicals were selected based on the availability of *in vivo* PK data to allow an assessment of the IVIVE model employed. A listing of the chemicals, their class and usage information, and fulfillment of the selection criteria is provided in Table 1.

Reagents and chemicals. Microsomal preparations of baculovirus-infected insect cells (BD Supersomes) expressing recombinant human CYP (1A2, 2A6, 2B6, 2C8, 2C9, 2C18, 2C19, 2D6, 2E1, 2J2, 3A4, 3A5, 3A7) and UGT (1A1, 1A4, 1A6, 1A9, and 2B7) enzymes, 0.5 M potassium phosphate buffer (pH 7.4), 0.5 M Tris-HCl buffer (pH 7.5), NADPH regenerating system solutions A and B, UGT reaction mix solutions A and B, Sf9 insect cell control Supersomes, UGT insect cell (BTI-TN-5B1–4) control Supersomes, and pooled human liver microsomes (HLMs; mixed gender 150 donor pool) were purchased from BD Biosciences (Woburn, MA). Acetonitrile, dimethyl sulfoxide, formic acid, and ammonium acetate were obtained from Sigma-Aldrich (St Louis, MO). Positive control chemicals and internal standards were purchased in neat form. Vendor and purity information for study chemicals, positive controls, and internal standards can be found in Supplementary tables 1A, B, and C, respectively.

Measurement of plasma and microsomal protein binding. Plasma protein binding was previously measured for each chemical (Wetmore *et al.*, 2012). Microsomal protein binding was determined for each chemical using the rapid equilibrium dialysis (RED) method with slight modification (Wetmore *et al.*, 2012). HLM (150-donor pool, equal gender mix; BD Biosciences) were rapidly thawed in a 37°C water bath and placed on wet ice prior to diluting to the concentration used in the assay (1 mg/ml, in 0.1 M potassium phosphate buffer). Chemicals were added to HLM (10 μM final concentration, in acetonitrile) and transferred in triplicate to the red chambers of the 96-well RED plate (catalog no. 90006, Thermo Fisher, Rockford, IL). White chambers were preloaded with 0.1 M potassium phosphate buffer. The RED plate was wrapped in aluminum foil and incubated at 37°C at 100 oscillations per minute for 4 h. After incubation, aliquots were removed and equal volumes of potassium phosphate buffer or HLM were added to aliquots from the HLM or potassium phosphate buffer chambers, respectively, for matrix matching. The samples were diluted with three times the volume of 100% acetonitrile. Excess undialyzed samples were transferred to polypropylene tubes, combined with an equal volume of potassium phosphate buffer, and three times the volume of 100% acetonitrile to assess non-specific binding of chemical to the RED plate. All samples were stored at <−70°C until analysis.

Measurement of recombinant CYP or UGT isozyme clearance rates. For each chemical, two master 96-well incubation plates (total well volume = 0.15 ml) containing potassium phosphate (0.1 M final concentration) or Tris (0.1 M, for CYPs 2C9 and 2A6) buffer, purified water, recombinant CYP or UGT isozyme, and chemical [1 and 10 μM final concentration with solvent (acetonitrile) concentration not to exceed 2% v/v] were prepared (Chauret *et al.*, 1998). Each chemical-isozyme sample was run in triplicate. Supersomes were added to the plate prior to chemical to minimize binding of chemical to plastic known to occur in the absence of protein. Plates were incubated at 37°C in a shaking water bath both prior to and after the addition of the appropriate regenerating system to start the reaction (NADPH system used for CYPs (final concentration of 1.3 mM $NADP^+$, 3.3 mM glucose-6-phosphate, 0.4 U/ml glucose-6-phosphate dehydrogenase, 3.3 mM $MgCl_2$); UGT reaction mix used for UGTs (final concentration of 50 mM Tris-HCl buffer (pH 7.5) containing 8 mM $MgCl_2$, 25 μg/ml alamethicin, and 2 mM UDPGA)). At 0, 5, 15, 30, and 60 min, a set volume (25 μl) was removed from the master plate and transferred to a collection plate containing an equal volume of acetonitrile to terminate the reaction. The collection plates were then shaken to mix the solution, sealed, and placed on ice prior to centrifugation at 2000 × g for 5 min and subsequent storage at <−70°C.

For each isozyme, positive control reactions were run in parallel and in duplicate to confirm the assay was functioning properly. The P450 content of the CYP enzymes was selected based on assay qualification information to allow for optimal detection of loss of parent chemical (BD Biosciences, unpublished communication) and ranged from 25–200 pmol/ml reaction volume. All UGT isozymes and HLMs were analyzed at 0.5 mg/ml. Where available, P450 isozyme products containing recombinant cytochrome b5 were used (Crewe *et al.*, 2011; Venkatakrishnan *et al.*, 2000). Supplementary table 1B contains detailed information including P450 content, protein concentration, positive control information, cytochrome B5 content, and activity information for each isozyme assessed. Negative controls containing Sf9 insect cell Supersomes (lacking detectable P450 content) or UGT insect cell control Supersomes (lacking detectable 7-hydroxy-4-trifluoromethylcoumarin glucuronidation activity) were run in parallel, with reactions terminated at 5 min and 60 min after initiation. Negative controls lacking regenerating system were also run. Similar results were obtained for both negative controls (data not shown).

Chemical analysis by liquid chromatography with mass spectrometric detection. Estimation of intrinsic metabolic clearance was estimated using substrate depletion, with loss of parent compound monitored over time. Samples from the metabolic stability assay (quenched 1:1 with acetonitrile) were thawed at room temperature and centrifuged at 3220 × g for 3 min. Samples were diluted with either 10 mM ammonium acetate in H_2O (pH = 7.4) or 0.1% formic acid (pH = 2.7) in H_2O. The 10 μM and 1 μM metabolic stability incubations were diluted 1:6. Prior to analysis, samples were spiked with internal standard and adjusted through the addition of acetonitrile to contain approximately 40% total organic content to match the initial chromatographic conditions described below. Internal standards were selected from a library of available compounds, with each internal standard being paired to its analyte based on the following parameters: (1) functional group similarities, (2) log D profile, and (3) pKa. Assessments revealed that the glucuronidated products formed were stable out to 48 h at 4°C. Samples were analyzed using an Agilent 6460 triple quadrupole mass spectrometer with an Agilent 1290 Infinity UHPLC system (Agilent, Santa Clara, CA). Calibration standards were prepared on the same day as sample analysis and in a matrix identical to the samples.

Samples from the microsomal protein binding assay (quenched 1:1:6, HLM:potassium phosphate buffer:acetonitrile)

TABLE 1. Background on Chemicals Analyzed

Chemical	Class/use pattern	Exposure information	*In vivo* PK data
Acetochlor	Chloroacetanilide herbicide (pre- and early post-emergent; corn)	Yes	No
Azoxystrobin	Strobilurin fungicide (grains, herbs, brassica vegetables)	Yes	No
Bensulide	Organophosphate herbicide (fruiting/leafy vegetables; homeowner use)	Yes	No
Carbaryl	Carbamate insecticide (apples, pecans, grapes; homeowner use)	Yes	Yes
Difenoconazole	Conazole fungicide (apples, barley, brassica vegetables, pecans)	Yes	No
Fludioxonil	Pyrrole fungicide (citrus, apple, root vegetables)	Yes	No
Haloperidol	Dopamine agonist (anti-psychotic drug)	No	Yes
Lovastatin	HMG-CoA reductase inihibitor (hypolipidemic agent)	No	Yes
Tebupirimfos	Organophosphate insecticide (corn)	Yes	No

were thawed at room temperature, vortexed briefly, and centrifuged at 6000 × g for 4 min. Sample preparation for the protein binding assay was identical to the metabolic stability assay described above.

Chromatographic separation was conducted on a Kinetex 1.7 μm XB-C18 100-Å column (Kinetex XB-C18, 50 mm × 2.1 mm, 1.7 μm) (Phenomenex, Torrance, CA) with a C_{18} guard column. Aqueous mobile phases used for these analyses were 0.1% formic acid (pH = 2.7) for positive ionization and 10 mM ammonium acetate (pH 7.4), for positive or negative ionization, with the organic phase being acetonitrile. Chromatographic separation was conducted using the following gradient conditions: (1) 40% organic for 0.1 min, (2) linear gradient ramp to 100% organic over 3.4 min, (3) maintain 100% organic for 0.1 min, (4) linear gradient ramp to 40% organic over 0.3 min, and (5) maintain 40% organic for 0.1 min. Total analysis time was 4.1 min per sample. The flow rate used for this analysis was 500 μl per min. Mass spectrometry conditions for all compounds are described in Supplementary table 1C.

Plasma and microsomal protein binding data analysis. To calculate the fraction of chemical unbound in the microsomal preparation (f_{umic}), the test compound concentration in the chamber containing buffer only was divided by the chemical concentration in the chamber containing microsomal protein. The fraction of chemical unbound in plasma (f_u) was obtained from an earlier study (Wetmore *et al.*, 2012). Data are provided in Supplementary tables 2A and B.

Recombinant CYP and UGT clearance data analysis. Substrate depletion was utilized to measure Cl_{int} in place of separate assessment of V_{max} and K_m, applying the use of first-order rate constants (Hallifax *et al.*, 2010; Lipscomb and Poet, 2008; Wetmore, 2014; Wetmore *et al.*, 2012). For each isozyme and each chemical, the percent of chemical remaining data at each time point is provided in Supplementary table 2C. The semi-log data were analyzed using linear regression. With three replicates at each of the five time points, a standard F-test (degrees of freedom = 1, 13; α = 0.10) was used to determine whether the slope of the line was significantly different from zero. In instances where the chemical amount fell below the limits of detection (LOD) before the completion of the time course, a value equivalent to the $LOD/\sqrt{2}$ was entered for the first time point at which the chemical was not detected (Hornung and Reed, 1990). The LOD values were calculated by dividing the concentration of the lowest standard by the root-mean-square signal-to-noise ratio then multiplying by 3. The intrinsic clearance derived for each recombinant enzyme ($Cl_{int\ rCYP}$ or $Cl_{int\ rUGT}$) was normalized to P450 content or protein content for rUGTs, with units of μl/(min × pmol P450) or μl/(min × mg protein).

Although the insect Sf9 and BTI-TN-5B1-4 cells used to express the recombinant CYP and UGT isozymes possess no detectable P450 content or 7-hydroxy-4-trifluoromethylcoumarin glucuronidation activity, respectively, other native enzyme activities present in these cells may elicit additional clearance of the parent compound. Insect cells possess carboxylesterase activity, which does not require the presence of any additional cofactors (Jamroz *et al.*, 2000; Whyard *et al.*, 1994). Any such background clearance was determined based on the natural log of the percent remaining at the 60 min time point in the appropriate negative control reactions and normalized to protein content using the following equation:

$$\text{Background clearance} = \frac{\ln(2)}{\left(T1/2 * \text{P450 content}\left(\text{pmol}/1000\ \mu\text{l}\right)\right) * \frac{\text{isozyme protn. conc}\left(\frac{\text{mg}}{\text{ml}}\right)}{\text{control SS protn. conc}\left(0.5\ \frac{\text{mg}}{\text{ml}}\right)}},$$

where

$$T_{1/2} = \frac{\ln(2) * (\text{incubation time})}{\ln((\%\ \text{remaining})/100)}.$$

This value was subtracted from the clearance rate derived for each isozyme $Cl_{int\ rCYP}$ value. An isozyme-chemical combination whose slope was not significantly different from zero ($p > 0.10$) and for which the isozyme-positive control reaction run in parallel displayed significant clearance was assigned a metabolic clearance of zero.

The unbound intrinsic clearance rate ($Clu_{int\ rCYP}$) was then calculated using the following equation:

$$Clu_{int\ rCYP} = \frac{Cl_{int\ rCYP}}{fu_{mic\ rCYP}}.$$

Fu_{mic} was determined in incubations of HLMs at protein concentrations of 1 mg/ml. These were scaled according to protein concentrations in the recombinant assays as follows:

$$fu_{mic\ rCYP} = \frac{1}{\left(\left(\frac{\text{rCYP assay protn. conc.}}{fu_{mic}\ \text{assay protn. conc. (HLM)}}\right) * \left((1 - fu_{mic\ HLM})/fu_{mic\ HLM}\right) + 1\right)}.$$

Estimation of subpopulation-based C_{ss} using intersystem extrapolation factor, IVIVE, and Monte Carlo simulation. The isozyme-specific clearance ($Cl_{int\ rCYP}$) and $fu_{mic\ assay}$ data were entered into the Simcyp simulation tool (Simcyp V. 11.1; Certara, Sheffield, UK) and used to estimate clearance using intersystem extrapolation factors (ISEFs) for CYPs and tissue scalars for UGTs (Crewe *et al.*, 2011; Proctor *et al.*, 2004). ISEFs are dimensionless scalars that are required to appropriately scale *in vitro* recombinant enzyme data to reflect whole organ metabolic clearance. ISEFs adjust for intersystem differences including lipid:protein ratios, nonspecific binding, and differences in CYP:NADPH CYP reductase:cytochrome b5 ratio (Crewe *et al.*, 2011; Lipscomb and Poet, 2008).

The ISEFs also adjust for differences in isoform abundance per mg microsomal protein. In a subsequent step, Simcyp derives population-specific metabolic clearance rates and related PK parameters by varying the abundance of the various CYP isozymes in the human liver, kidney, or intestine (pmol/mg protein) such that they correspond to the concentrations for a particular individual or subpopulation of interest. As sufficient data are not yet available to calculate ISEFs for UGTs, a tissue scalar or relative activity factor approach is used to relate expression and activity of the UGT in the recombinant enzyme to that of the native enzyme in the microsomes from the tissue of interest (Gibson *et al.*, 2013). For UGTs, variability in relative abundance (rather than absolute abundance) is factored into the scaling of clearance. Tissue scalar information is provided in Supplementary table 3A.

The chemical steady-state blood concentrations (C_{ss}) were estimated using the following equation. The equation is based on constant uptake of a daily oral dose and factors in plasma protein binding, hepatic clearance, metabolic and nonmetabolic renal clearance, and intestinal clearance:

$$C_{SS} = \frac{ko}{\left(\frac{(Q_H \times F_{ub} \times Cl_{int\,H})}{(Q_H + F_{ub} \times Cl_{int\,H})}\right) + \left(\frac{(Q_R \times F_{ub} \times Cl_{int\,R})}{(Q_R + F_{ub} \times Cl_{int\,R})} + GFR \times F_{ub}\right) + \left(\frac{Q_G \times F_{ub} + Cl_{int\,G}}{Q_G + F_{ub} \times Cl_{int\,G}}\right)}$$

where ko = chemical exposure rate set to 0.042 mg/kg/h (i.e., 1 mg/kg/day); F_{ub} = unbound fraction of parent compound in the blood; GFR = glomerular filtration rate; Q_H, Q_R, Q_G = hepatic, renal, or intestinal blood flow, respectively; and Cl_{intH}, Cl_{intR}, Cl_{intG} = hepatic, renal, or intestinal intrinsic metabolic clearance, respectively. The F_{ub} was calculated based on the experimentally measured $F_{u\ plasma}$ divided by the blood:plasma ratio (B:P). The CL_{int} values were derived by scaling experimentally measured $CLu_{int\ rcyp}$ rates to represent whole organ clearance by factoring in microsomal protein per gram tissue (MPPGL for the liver, MPPGK for the kidney) or microsomal protein per total intestine (MPPI), and the volume (in g) of the respective tissues.

Non-metabolic renal clearance (GFR × F_{ub}) also varied in accordance with the specific subpopulation of interest. The GFRs for the adult subpopulations were backcalculated based on the serum creatinine Cockcroft-Gault equation (Cockcroft and Gault, 1976). Compared with the healthy adult 20–50-year-old population, median GFRs were 4% lower in female 20–50 year olds, 37% lower in 50–80 year olds, and 80% lower in renally-compromised populations. For the pediatric subpopulations, the GFRs were calculated using a body surface area-based equation developed from a meta-analysis of studies investigating age-based changes in GFR (Johnson *et al.*, 2006). Compared with the healthy adult population, the median GFRs for the newborn to 6 month-old and 1 to 6-year-old groups are 91 and 70% lower, respectively (Rubin *et al.*, 1949). GFRs applied for all populations are provided in Supplementary table 3A.

Both healthy and general adult population Simcyp libraries were employed (Dickinson and Rostami-Hodjegan, 2008). The healthy adult population was used as the comparator in this study and is comprised of North European Caucasian adults who have taken part in phase I clinical studies. The other Simcyp population libraries have been built from public health databases, particularly the US National Health and Nutrition Examination Survey (NHANES) database and census data produced by UK and Japanese governmental bodies, as well as extensive meta-analyses of numerous literature sources (Howgate *et al.*, 2006; Jamei *et al.*, 2009). Consequently, the North European Caucasian, Japanese, and Chinese population libraries represent general rather than healthy populations, as it is difficult to define a healthy population and surveys do not usually separate healthy individuals from those with minor health issues and those with major health issues or diseases. Two sets of subpopulations were assessed.

The first set of populations was defined based on known PK and physiologic differences across age groups identified in pediatric pharmacology and developmental ontogeny studies (Cresteil, 1998; Hines, 2007; Kearns *et al.*, 2003). These populations included multiple life stages [0–0.5 years, 0.5–2 years, 2–6 years, 6–20 years, and 20–50 years (Healthy)], ethnic backgrounds (Chinese, Japanese, and North European Caucasian), and chronic diseases (diabetes and compromised renal function). Both sexes were included in all of the populations. In the populations broken out by life stage and chronic disease, the ethnic background was North European Caucasian. In the populations broken out by ethnic background and chronic disease, the age range was 20–50 years of age.

The second set of populations was defined to allow direct comparison with life stage-based exposure estimates collated from US Environmental Protection Agency (US EPA) exposure estimates. These populations included different age ranges [<1 yr, 1–2 years, 3–5 years, 6–12 years, 20–50 years (Healthy); and 50 – 80 years] and females of reproductive age (16–49 years). In the populations broken out by life stage, both sexes were included and the ethnic background was North European Caucasian. For the females of reproductive age, the ethnic background was North European Caucasian. For all of the populations assessed, Simcyp provides pre-parameterized libraries except for the female (16–49 years old) and the 50–80-year-old subgroups. However, given that patient characteristics that would impact the C_{ss} determinations such as microsomal protein per gram tissue, tissue blood flows and tissue volumes vary for these subpopulations and are captured within Simcyp during the simulations, selection for these particular gender- and age-based subpopulations from the default population library (i.e., the North European Caucasian library) still provides useful information about the PK differences for these two subpopulations for this analysis. A correlated Monte Carlo approach (Jamei *et al.*, 2009) was used to simulate variability across 10,000 individuals in each subpopulation. The median, upper, and lower fifth percentiles for the C_{ss} were obtained as output.

In vitro bioactivity data. The ToxCast program measured biological activity across >600 *in vitro* assay endpoints using nine separate technologies including receptor-binding and enzyme activity assays, cell-based protein and RNA expression assays, real-time growth measured by electronic impedance, and fluorescent cellular imaging. Each chemical-assay combination was run in

dose response and an AC_{50} or LEC value was estimated depending on the range of the dose response data. The *in vitro* bioactivity was assumed to be solely the result of the parent compound. Although two assays used primary hepatocyte cultures with some metabolic capacity, most of the assays lacked known metabolic activity. A detailed description of the assays and associated data are provided in earlier publications (Houck *et al.*, 2009; Huang *et al.*, 2011; Judson *et al.*, 2010; Knight *et al.*, 2009; Knudsen *et al.*, 2011; Martin *et al.*, 2010; Rotroff *et al.*, 2010a). All *in vitro* HTS data are available from the ToxCast web site (http:/www.epa.gov/ncct/toxcast).

Calculation and statistical presentation of oral equivalent dose values data. In conventional use, PK models are used to relate exposure concentrations to a blood or tissue concentration. This is typically referred to as "forward dosimetry". In contrast, the models can also be reversed to relate blood or tissue concentrations to an exposure concentration, which is referred to as "reverse dosimetry" (Tan *et al.*, 2007). As previously described, the *in vitro* AC_{50} or LEC values were assumed to be functionally equivalent to the C_{ss} values in terms of biological activity (Rotroff *et al.*, 2010b; Wetmore *et al.*, 2012). Based on the principal of reverse dosimetry, the median, 5th, and 95th percentiles for the C_{ss} were used as conversion factors to generate oral equivalent doses according to the following formula:

$$\text{Oral equivalent}\left(\frac{\frac{\text{mg}}{\text{kg}}}{\text{day}}\right) = \text{Tox Cast } AC_{50} \text{ or LEC}(\mu\text{M}) \times \frac{1\frac{\frac{\text{mg}}{\text{kg}}}{\text{day}}}{C_{ss}(\mu\text{M})}.$$

In the equation above, the oral equivalent dose value is linearly related to the *in vitro* AC_{50} or LEC and inversely related to C_{ss}. Two sets of C_{ss} values were obtained using *in vitro* clearance data measured at the tested chemical concentrations (1 and 10μM). The C_{ss} output selected to calculate the oral equivalent for each chemical-assay combination corresponded to that which utilized clearance rates derived at the chemical concentration closest to the AC_{50} or LEC value for that assay (Rotroff *et al.*, 2010b; Wetmore *et al.*, 2012). This equation is valid only for first-order metabolism that is expected at ambient exposure levels. An oral equivalent value was generated for each chemical and each AC_{50} or LEC value across the 600 *in vitro* assay endpoints. Those chemical and assay combinations that did not show activity (i.e., did not possess an AC_{50} or LEC value) were not simulated.

Box and whisker plots were used to visualize the oral equivalent dose values for each chemical. In each figure, the 95th percentile of the C_{ss} was used in the figures to provide a conservative estimate of the oral equivalent dose values. The median oral equivalent dose value for each chemical was displayed as a horizontal line and the ends of the boxes represent the 25th and 75th percentiles. The whiskers denote those values that fall either less than or greater than 1.5 times the interquartile range from the 25th or 75th percentiles, respectively (Tukey, 1977). In those instances where the minimum or maximum value for that chemical does not exceed the whisker, the whisker is set to that value. Any value beyond the range of the whiskers is designated as an outlier and is displayed as a black circle.

Evaluation of PK modeling. Published studies of the human *in vivo* PKs of carbaryl (May *et al.*, 1992), haloperidol (Mihara *et al.*, 1999; Suzuki *et al.*, 2003; Yasui-Furukori *et al.*, 2002), and lovastatin (Bramer *et al.*, 1999; Kothare *et al.*, 2007; Mignini *et al.*, 2008) were used to estimate the human plasma C_{ss} given an oral exposure of 1 mg/kg/day. These values were then compared against the IVIVE-derived values generated using the *in vitro* isozyme-specific clearance rates.

Relative impact of physiology versus enzyme clearance rates to population variability. To separate out the contribution of physiologic differences from metabolic differences in human toxicokinetic variability, the following steps were taken. First, IVIVE was performed using *in vitro* isozyme-specific clearance data to estimate *in vivo* Cl_{int}. Output obtained included estimations of *in vivo* hepatic, renal, and intestinal clearance. Next, these *in vivo* hepatic, renal, and intestinal clearance rates were adjusted with a scaling factor to predict *in vitro* hepatic, renal, and intestinal clearance rates that would yield the same *in vivo* clearance values (i.e., performing an *in vivo* to *in vitro* scaling). The resulting *in vitro* clearance rates were input into a subsequent IVIVE in place of the isozyme-specific clearance rates to derive the C_{ss} output, whereas the population libraries were varied. This variation at the population library level would incorporate differences in tissue weights, tissue blood flow (e.g., hepatic, intestinal, and renal blood flow), body weights, etc. without the adjustment for isozyme abundances as performed when the isozyme clearance rates were used. Simulations were conducted using the healthy adult and the most sensitive subpopulations for each chemical. The resulting C_{ss} values provide an assessment of the impact of population-based differences in physiology on population variability. Clearance rates, scaling factors, and findings are provided in Table 4 and Supplementary tables 3C and D.

Human oral exposure estimates. Exposure estimates were obtained from available EPA Office of Pesticide Programs documents and Federal Register notices. The majority of the estimates came from Reregistration Eligibility Documents that contained residue levels and estimated aggregate exposures from food and drinking water sources organized by various age groups and subpopulations. These estimates were collated previously (Wetmore *et al.*, 2012) and have been confirmed to be up to date for this study.

RESULTS

Assessment of Isozyme-Specific Clearance

In this study, metabolic clearance assays were conducted for 13 CYP and 5 UGT isozymes at 1 and 10 μM chemical concentrations. The 1 μM concentration is typically used in rCYP-based clearance assays conducted in the pharmaceutical industry as this concentration is believed to be significantly below the K_m for most compounds (Harper and Brassil, 2008; Stringer *et al.*, 2009), whereas both 1 and 10 μM concentrations fall in the middle of the range of concentrations tested in the ToxCast assays. IVIVE simulations incorporating these data were used to calculate the fraction of compound metabolized (fm), which takes into account isozyme-specific clearance rates along with isozyme abundance to assess the overall contribution of each isozyme to chemical clearance. When using the healthy adult population library, simulations revealed that CYPs 1A2, 2C9, and 3A4 and UGT1A4 were main contributors to clearance for three to seven of the nine compounds assessed (Table 2). CYP3A4 was a major contributor to metabolism, accounting for

TABLE 2. Summary of Percent Contribution of Isozymes to Chemical Clearance

Isozyme[a]	Population	No. of chemicals with percent fm > 5%[a]	Percent fm range[b]	Chemicals where percent fm > 5%
CYP1A2	Healthy adult	3	4.71 (0.4–91.36)	Bensulide, carbaryl, fludioxonil
	Pediatric (0–0.5)	2	1.55 (0.2–75.35)	Carbaryl, fludioxonil
CYP2B6	Healthy adult	1	2.30 (0.3–10.28)	Acetochlor
	Pediatric (0–0.5)	1	0.63 (0.17- 7.60)	Acetochlor
CYP2C8	Healthy adult	0	0.31 (0.26–3.81)	None
	Pediatric (0–0.5)	1	0.77 (0.6 - 5.6)	Tebupirimfos
CYP2C9	Healthy adult	6	5.41 (2.05–63.08)	Azoxystrobin, bensulide, carbaryl, difenoconazole, haloperidol, tebupirimfos
	Pediatric (0–0.5)	8	17.96 (4.66–77.03)	Acetochlor, azoxystrobin, bensulide, carbaryl, difenoconazole, haloperidol, tebupirimfos
CYP2C18	Healthy adult	0	0.02 (0.01–0.18)	None
	Pediatric (0–0.5)	0	0.02 (0.01–0.16)	None
CYP2C19	Healthy adult	2	1.08 (0.03–24.50)	Bensulide, tebupirimfos
	Pediatric (0–0.5)	3	1.82 (0.05–22.64)	Azoxystrobin, bensulide, tebupirimfos
CYP2D6	Healthy adult	0	0.31 (0.11–0.85)	None
	Pediatric (0–0.5)	0	0.39 (0.12–1.47)	None
CYP2E1	Healthy adult	0	0.76 (0.22–1.71)	None
	Pediatric (0–0.5)	0	1.55 (0.26–2.78)	None
CYP2J2	Healthy adult	0	0.07 (0.05–0.27)	None
	Pediatric (0–0.5)	0	0.20 (0.08–0.44)	None
CYP3A4	Healthy adult	7	43.30 (0.97–80.19)	Acetochlor, azoxystrobin, bensulide, difenoconazole, haloperidol, lovastatin, tebupirimfos
	Pediatric (0–0.5)	7	28.49 (1.20–64.42)	Same as above
CYP3A5	Healthy adult	2	2.95 (1.37–6.36)	Lovastatin, tebupirimfos
	Pediatric (0–0.5)	3	4.35 (2.33–8.90)	Acetochlor, lovastatin, tebupirimfos
CYP3A7	Healthy adult	0	0.11 (0.01–0.46)	None
	Pediatric (0–0.5)	2	1.66 (0.12–5.84)	Lovastatin, tebupirimfos
UGT1A1	Healthy adult	2	5.83 (2.59–19.33)	Haloperidol, tebupirimfos
	Pediatric (0–0.5)	2	5.72 (3.71–28.69)	Same as above
UGT1A4	Healthy adult	3	4.55 (0.11–12.06)	Difenoconazole, haloperidol, lovastatin
	Pediatric (0–0.5)	4	9.45 (0.13–19.97)	Acetochlor, difenoconazole, haloperidol, lovastatin
UGT1A9	Healthy adult	1	3.74 (2.16–9.26)	Carbaryl
	Pediatric (0–0.5)	1	1.43 (1.13–8.00)	Carbaryl
UGT2B7	Healthy adult	1	19.67 (4.39–34.96)	Haloperidol
	Pediatric (0–0.5)	1	5.33 (0.73–9.94)	Haloperidol

[a]Simulations were performed using $Cl_{in\ vitro}$ measured at 1μM.
[b]Median, with minimum to maximum values in ().

TABLE 3. Comparison of IVIVE Modeling Results with Published *in vivo* PK Data

Chemical	Population	*In vivo* PK C_{ss} (μM)[a]	IVIVE C_{ss} (μM)[a,b]
Carbaryl	Healthy adult	0.03	0.043
Haloperidol	Japanese	0.090–0.126	0.029
Lovastatin	Healthy adult	0.004–0.009	0.001

[a]C_{ss}, steady-state blood concentration for 1 mg/kg/day dose.
[b]Predicted using the 1 μM metabolic clearance rate.

65–80% of the clearance for four of the nine chemicals (Table 2). All UGT isozymes glucuronidated at least one chemical with an fm exceeding 5%, with the median fm range spanning 3.7% to 19.7%. When using the pediatric (0–0.5 years) life stage population a similar trend was observed, although CYP2C9 contributed to clearance of eight of the nine compounds compared to seven for CYP3A4. In addition, pediatric CYP3A7 displayed fm values exceeding 5% for two chemicals. A complete breakdown of fm data across all chemicals and isozymes for these two populations is provided in Supplementary table 4.

TABLE 4. Estimated Chemical-Specific Toxicokinetic Adjustment Factors (HK_{AFs}) Using the IVIVE Modeling Results

	1μM				10μM				
Chemical	Median C_{ss} healthy population[a]	95th percentile (median) C_{ss} most sensitive[b]	Most sensitive	Estimated HK_{AF}[c] 95th:median (median: median)	Median C_{ss} healthy population[a]	95th percentile (median) C_{ss} most sensitive[b]	Most sensitive	Estimated HK_{AF}[c] 95th:median (median: median)	Average estimated HK_{AF}[d]	Percent contribution of isozyme differences to average HK_{AF}
Acetochlor	0.026	0.17 (0.063)	Pediatric (0–0.5)	6.7 (2.5)	0.064	0.24 (0.10)	Pediatric (0–0.5)	3.7 (1.6)	5.2 (2.0)	80
Azoxystrobin	0.099	0.66 (0.22)	Pediatric (0–0.5)	6.7 (2.2)	0.64	5.53 (1.63)	Pediatric (0–0.5)	8.6 (2.5)	7.7 (2.4)	86
Bensulide	0.241	0.97 (0.35)	Pediatric (0–0.5)	4.0 (1.5)	5.58	21.43 (9.58)	Renal Failure	3.8 (1.7)	3.9 (1.6)	66
Carbaryl	0.043	0.49 (0.17)	Pediatric (0–0.5)	11.4 (4.0)	0.062	0.92 (0.28)	Pediatric (0–0.5)	14..8 (4.5)	13.1 (4.3)	88
Difenoconazole	0.201	0.71 (0.30)	Renal Failure	3.5 (1.5)	0.718	2.16 (0.79)	Chinese	3.0 (1.1)	3.3 (1.3)	58
Fludioxonil	0.380	4.37 (1.45)	Pediatric (0–0.5)	11.5 (3.0)	1.672	16.81 (5.98)	Pediatric (0–0.5)	10.1 (3.6)	10.8 (3.3)	86
Haloperidol	0.029	0.14 (0.04)	Pediatric (0–0.5)	4.9 (1.5)	0.033	0.16 (0.06)	Pediatric (0–0.5)	4.8 (1.8)	4.8 (1.6)	83
Lovastatin	0.001	0.009 (0.003)	Pediatric (0–0.5)	6.5 (2.1)	0.001	0.01 (0.002)	Pediatric (0–0.5)	10.1 (2.2)	8.3 (2.2)	92
Tebupirimfos	0.107	0.38 (0.16)	Renal Failure	3.5 (1.5)	0.054	0.14 (0.06)	6 to 20 years	2.6 (1.1)	3.1 (1.3)	20

[a]Median C_{ss} values estimated using Monte Carlo simulation for healthy adult (20–50 years) population (see the Materials and Methods section).
[b]Upper 95th percentile and median (in parentheses) C_{ss} values estimated for the most sensitive population (i.e., population with the highest 95th percentile value for that chemical).
[c]Estimated human toxicokinetic adjustment factors (HK_{AF}) calculated from the ratio of (1) the 95th percentile C_{ss} for the most sensitive to the median of the healthy population (95th percentile:median) or (2) the median for the most sensitive to the median of the healthy population (in parentheses; median:median).
[d]Average of the 1- and 10-μM HK_{AFs}.

Generation and Assessment of Subpopulation-Specific C_{ss} Values

Median, 5th, and 95th percentile C_{ss} values were collated from simulations conducted across multiple life stages and ethnic- and disease-based populations using *in vitro* chemical clearance rates at the 1 μM concentration (Fig. 2). Generally, those chemicals cleared by multiple isozymes displayed the least variability across subpopulations, whereas carbaryl, cleared by only two isozymes, displayed the greatest (Figs. 2A and B and Table 3). Among the life stage-based populations, the pediatric group (0–0.5 years) typically showed the highest C_{ss} values. Although the subchronic disease subpopulations showed C_{ss} values as higher than the highest ethnic subpopulation, they were generally lower than the youngest pediatric life stage. For most of the chemicals, the C_{ss} values derived at the 10-μM chemical clearance rates displayed a similar trend (data not shown). A complete listing of all of the estimated C_{ss} values is provided in Supplementary table 3B.

Evaluation of IVIVE Modeling

Three of the nine chemicals analyzed had *in vivo* PK studies available in the literature from which C_{ss} values could be derived (Table 3). These chemicals included carbaryl, haloperidol, and lovastatin. A single *in vivo* PK study was available for carbaryl with an estimated C_{ss} value of 0.03μM for a 1-mg/kg/day dose (May *et al.*, 1992). The IVIVE-predicted median C_{ss} value for carbaryl was 0.046 μM and within 1.5-fold of the *in vivo* PK-derived value. For haloperidol, *in vivo* C_{ss} values were calculated from three published studies (Mihara *et al.*, 1999; Suzuki *et al.*, 2003; Yasui-Furukori *et al.*, 2002) and were within 1.4-fold of each other (0.09–0.126 μM). The IVIVE-derived value for haloperidol was 0.0285 μM, falling 3.2–4.4-fold lower than the *in vivo* PK-derived values. Three published studies were used to estimate the lovastatin *in vivo* PK C_{ss} values (Bramer *et al.*, 1999; Kothare *et al.*, 2007; Mignini *et al.*, 2008). The three *in vivo* studies resulted in a 2.5-fold range of C_{ss} values between 0.004 and 0.009μM, whereas the IVIVE-derived value of 0.001μM was 4–9-fold lower, depending on the study.

Estimation of Chemical-Specific Human Toxicokinetic Adjustment Factors (HK_{AF})

Two methods were used to derive chemical-specific HK_{AFs} to account for inter-individual variability. These methods divided either (1) the 95th percentile or (2) the median value for the sensitive population by the median value for the general healthy population. The 95th:median ratio HK_{AF} is consistent with a strategy previously outlined to convey toxicokinetic variability for a bimodal population and is based on the assumption that a sensitive subpopulation is a discrete group rather than a fraction of the general population (Lipscomb *et al.*, 2004). For the chemicals evaluated, the average estimated 95th:median and

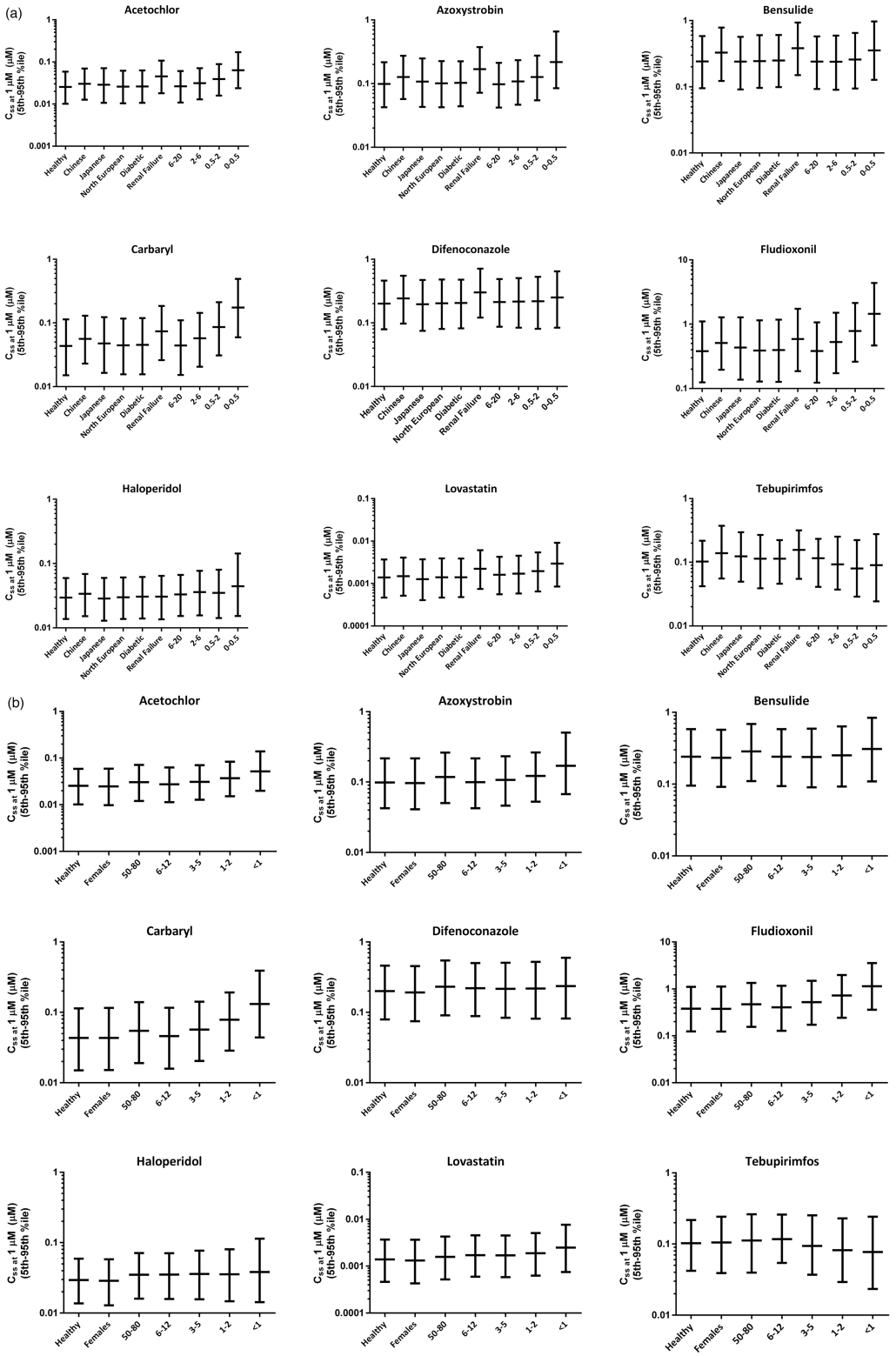

FIG. 2. Comparison of C_{ss} values derived across multiple subpopulations. 5th, median, and 95th percentile C_{ss} values are displayed in box and whisker format for the nine chemicals analyzed in the study. C_{ss} values were derived using hepatic clearance rates at 1µM chemical concentration. Non age-based subpopulations had an age range of 20–50 years of age, equal numbers of both genders, and were selected based on availability in the Simcyp simulation tool: Healthy, Chinese, Japanese, Northern European (Northern European Caucasian), Female, Diabetic, and Renal Failure (individuals with a glomerular filtration rate < 30 ml/min). For the remaining subpopulations, the numbers represent the age range (in years) simulated. Panel (A) displays life stage-, ethnic-, and disease-based subpopulations chosen due to characterization of PK and physiologic differences in meta-analyses and pediatric studies from varied literature sources. Panel (B) displays subpopulations simulated to allow direct comparison with age-based exposure estimates collated from regulatory documents. Additional information about subpopulations is available in the Materials and Methods section.

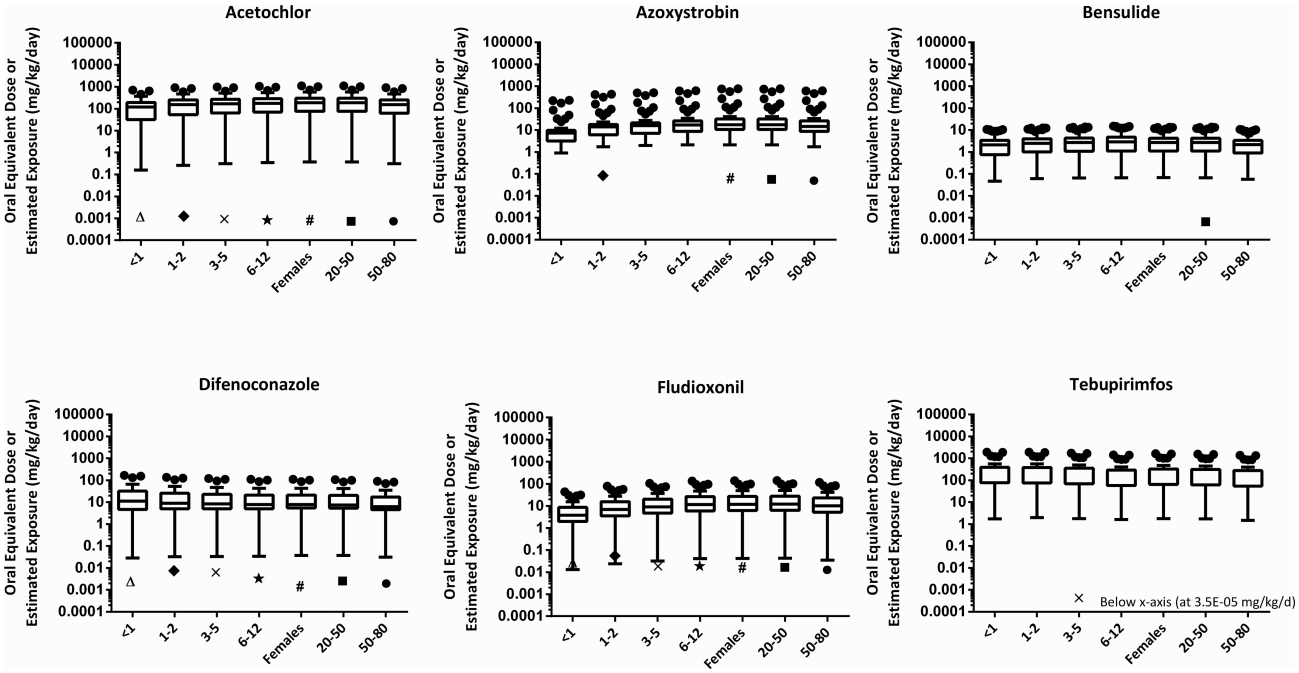

FIG. 3. Comparison of subpopulation-specific oral equivalent ranges and exposure estimates. Box and whisker plots depict the range of the oral equivalent values calculated for each chemical-subpopulation group with the lower and upper whiskers set to represent the range of values 1.5 times the interquartile range below or above the 25th or 75th percentiles, respectively. In those instances where the lowest or highest value for that chemical-assay combination does not exceed the whisker, the whisker is set to that value. Subpopulations are as defined in Figure 1. Symbols (Δ,◇,×,□,#,■,•) depicting human life stage-based oral exposure estimates derived from US regulatory documents are included where available.

median:median HK_{AFs} ranged from 3.1- to 13.1-fold and 1.3- to 4.3-fold, respectively (Table 4). Except for tebupirimfos, the average estimated 95th:median HK_{AFs} for all chemicals were greater than the default uncertainty factor of 3.2. In general, the most sensitive population was the youngest pediatric life stage group (pediatric 0–0.5 years). The chemicals with ethnic or chronic disease populations as the most sensitive had HK_{AF} values closer to the default uncertainty factor.

Relative Impact of Physiology Versus Enzyme Ontogeny to Subpopulation Variability

To assess the relative impact of age-based differences in physiology and metabolism on C_{ss}, model simulations were run for the healthy and most sensitive populations while holding the metabolic clearance rates constant. The percent contribution of subpopulation metabolic differences to the HK_{AF} values for all but tebupirimfos ranged from 58–92%, with six of the nine chemicals greater than 80% (Table 4 and Supplementary table 3C). For tebupirimfos, metabolic differences only accounted for 20% of the variability. In addition, comparison of the physiology-based median C_{ss} values for the most sensitive and healthy adult populations yielded healthy adult C_{ss} values that were higher than those for the most sensitive subpopulation for all but one chemical (tebupirimfos) (Supplementary table 3C).

Comparison of Subpopulation-Specific Oral Equivalent Doses to Subpopulation-Specific Oral Exposure Estimates

Subpopulation-specific C_{ss} values were used to estimate the subpopulation-specific oral equivalent doses for each chemical-assay combination. The subpopulations evaluated in this analysis were those selected based on exposure estimates collated from US EPA exposure estimates. Given that between 75 and 129 *in vitro* assays yielded AC_{50} or LEC values for the chemicals tested in this study, box and whisker plots were used to depict the range and distribution of the subpopulation-specific oral equivalent doses (Fig. 3). In most cases, the pediatric (0–0.5 years) life stage possessed the lowest minimum oral equivalent dose value among all subpopulations (denoted by the lower whisker).

To best capture the differences between the oral equivalent dose ranges and the exposure estimates, activity-to-exposure ratios (AERs) were calculated by dividing the lower whisker by the appropriate age-based exposure estimate (Supplementary table 5). One chemical, fludioxonil, had AERs for two pediatric subpopulations (<1 and the 1–2-year-old group) that were less than 1, indicating that the estimated exposures could lead to blood concentrations similar to those that elicited bioactivity in the *in vitro* HTS assays. The AERs were less than 3.3 for all of the other subpopulations for this chemical. Only two of the six other chemicals for which exposure estimates were available had AERs less than 100 for at least one of the subpopulations assessed—azoxystrobin (40, for the 1–2-year age group) and difenoconazole (values ranging from 7 to 25 for all age groups). On a chemical-by-chemical basis, the difference between the largest and smallest AERs ranged from 2.2 to 7.1-fold (Supplementary table 5).

DISCUSSION

Within the United States and abroad, consideration of uncertainty and variability is recognized as a critical part of the risk assessment process (EPA, 2005; Meek *et al.*, 2002). To address the uncertainty in predicting human effects from animal toxicity studies and the potential variability in response between general and more sensitive human populations, the US EPA applies default uncertainty factors in their non-cancer risk assessments to ensure the adequate protection of human health (NRC, 1983).

A greater understanding of species-specific and subpopulation-specific PK and pharmacodynamic differences has led regulators to consider transitioning away from these default values to data-driven, chemical-specific adjustment factors when appropriate (Dorne and Renwick, 2005; Lipscomb *et al.*, 2004). The US EPA and the International Programme for Chemical Safety have released draft guidance documents that provide frameworks for such an approach (IPCS, 2005) (Lipscomb *et al.*, 2004), whereas strategies that incorporate pathway-related uncertainty factors for chemicals with intermediate data availability have also been introduced (Dorne, 2010; Lipscomb *et al.*, 2004). Further, in 2009 a report released by the US National Research Council recommended implementing a tiered approach in determining the level of detail necessary to support uncertainty and variability assessments (NRC, 2009).

Over the past decade, the US EPA has been under increasing pressure to streamline hazard identification and prioritization of the thousands of chemicals in commerce for which limited or no toxicity data are available (EPA, 2003; Kavlock *et al.*, 2005). In response to this pressure, the US EPA ToxCast research program was launched in 2007 to incorporate *in vitro* HTS and bioinformatics tools into the process (Dix *et al.*, 2007; Judson *et al.*, 2010; Kavlock *et al.*, 2009). Since then, close to 1800 chemicals have been evaluated for their potential to perturb hundreds of pathways and biological processes *in vitro* (Houck *et al.*, 2009; Knight *et al.*, 2009; Knudsen *et al.*, 2011; Martin *et al.*, 2010; Rotroff *et al.*, 2010a). Previous studies have integrated PK with the *in vitro* HTS data to estimate oral equivalent doses that would result in steady-state blood levels equivalent to concentrations eliciting bioactivity in the *in vitro* assays (Rotroff *et al.*, 2010b; Wetmore *et al.*, 2012). The integration of PK has been critical for application to risk assessment (Judson *et al.*, 2011). The ability to incorporate subpopulation susceptibility into the generation of these oral equivalent doses would further enhance the applicability of the HTS data within a risk assessment framework.

In this study, metabolic clearance rates were measured for a subset of nine ToxCast chemicals across 13 CYP and 5 UGT isozymes. All nine chemicals were significantly cleared by at least one CYP and one UGT isozyme. Fm assessment revealed that CYPs 1A2, 2C9 3A4, and UGT1A4 played a major role in metabolizing the chemicals tested. These findings are consistent with reports in the pharmaceutical literature, where these four isozymes are the most abundantly expressed in hepatic tissue and are responsible for over 62% of drug metabolism (Donato and Castell, 2003; Pinto and Dolan, 2011; Singh *et al.*, 2011). Comparison of fms between pediatric (0–0.5 years) life stage and the adult population revealed similar trends, although CYPs 2C9 and neonatal 3A7 significantly metabolized (i.e., possessed fm >5%) more chemicals in this pediatric population. This observation is consistent with the more rapid development of CYP2C9 in the first few months of life compared with CYP3A4 (Johnson *et al.*, 2006; Koukouritaki *et al.*, 2004), and the decrease in CYP3A7 levels as development ensues and CYP3A4 levels increase (Hines, 2007). Although the UGTs are primarily recognized as a phase II enzyme family, they also glucuronidate unmodified compounds containing carboxylic acids, aminophenols, or other functional groups (Tukey and Strassburg, 2000). The phase I activity of UGTs was evident in this study, where several of the isozymes displayed broad substrate specificity by each glucuronidating five to six of the nine compounds tested (Supplementary table 4). Although CYPs and UGTs were selected for this study due to their recognized prominence in xenobiotic metabolism, other hepatic enzymes (e.g., flavin-containing monooxygenases, sulfotransferases) may also metabolize some of the chemicals tested. However, the CYPs and UGTs are also the only enzymes with sufficient isozyme abundance and developmental ontogeny data to allow the generation of subpopulation-specific C_{ss} values.

The isozyme-specific intrinsic clearances expressed per unit enzyme were used together with isozyme abundance data and known physiologic differences to construct IVIVE PK models for multiple subpopulations to predict chemical concentration in the blood at steady state. Use of rCYP and rUGT reaction phenotyping in such a model requires acknowledgment of certain details. First, incubations with recombinant enzymes are typically performed at enzyme levels that exceed physiologic levels to offer high assay sensitivity in detecting substrate depletion. In addition, in those instances where a chemical is a substrate for multiple enzymes, the differing kinetic behaviors (e.g., K_m, V_{max}) of each enzyme may impact the relative contribution of each to overall *in vivo* Cl_{int} in a manner that is not captured in these *in vitro* assessments (Harper and Brassil, 2008). However, a comparison of the performance of three *in vitro* systems in predicting *in vivo* Cl_{int} for 110 drugs revealed that recombinant enzymes outperformed hepatocytes and liver microsomes, providing predictions within 5-fold of the observed *in vivo* Cl_{int} for 70% of the chemicals (Stringer *et al.*, 2009).

To evaluate the accuracy of the IVIVE modeling, the IVIVE predictions were compared with C_{ss} values derived from published *in vivo* PK studies. The IVIVE model for carbaryl was within 1.5-fold of the *in vivo* value, whereas the IVIVE models for haloperidol and lovastatin were within 3-fold and 4–9-fold of the *in vivo* values, respectively. It should be noted that the two *in vivo* studies used to provide C_{ss} values for lovastatin also demonstrated variability, with C_{ss} estimates spanning 2.5-fold. Although three chemicals is a limited number to draw broad conclusions on the utility of the approach, the IVIVE-predicted C_{ss} values were generally comparable to C_{ss} values from the published models and come within the 3–5-fold range desired in sound IVIVE strategies (Hallifax *et al.*, 2010).

The measurement of isozyme-specific intrinsic clearance expressed per unit enzyme enables the use of IVIVE and incorporation of system-specific parameters in different virtual populations. One advantage of this "bottom-up" approach is that as data describing the demographic, genetic, and physiological data continue to emerge and evolve, revised system parameters can be incorporated and the likely exposure in relevant sensitive populations resimulated. For instance, UGTs 1A9 and 2B7 are present in the kidney (Fisher *et al.*, 2001; King *et al.*, 2000), and the intestine possesses UGT1A1 as well as the intestinal-specific UGTs 1A7, 1A8, and 1A10 (Fisher *et al.*, 2001; Gregory *et al.*, 2004; Ritter, 2007; Thelen and Dressman, 2009). This latter group of UGTs was not measured in our study. The measurement of UGT-mediated clearance and incorporation of rUGT:tissue scalars allows the incorporation of this extrahepatic metabolism into the modeling results. As absolute renal and intestinal UGT abundance data emerge in the literature for different populations, this approach can be further refined to incorporate Cl_{int} per pmol isozyme, thus replacing the tissue scalar approach.

Isozyme ontogeny data were derived from measurements of enzyme expression and activity from multiple studies and reported previously (Johnson *et al.*, 2006). Developmental differences in isozyme abundances were evaluated by applying a number of models, with the most parsimonious model identified and used to derive the fraction of adult CYP abundance for each age band (Johnson *et al.*, 2006). Several reports on CYP ontogeny in the literature suggest that a higher coefficient of variation (CV) exists within certain age bands, particularly around birth (Croom *et al.*, 2009; Hattis *et al.*, 2003; Johnsrud *et al.*, 2003; Kouk-

ouritaki *et al.*, 2004). As insufficient data are available to delineate the variability that exists due to the fast postnatal isozyme development from true isozyme variability, the approach within Simcyp applies CVs based on adult data across the whole pediatric age range (Rowland-Yeo *et al.*, 2003). From a risk assessment perspective, an alternate approach that accounts for greater CVs may need to be considered to ensure adequate protection of this sensitive life stage group.

The population-specific IVIVE models were applied in two different ways. The first application was to assess the range of variability in C_{ss} values across a broad range of populations and use the variability to estimate chemical-specific human toxicokinetic adjustment factors (HK_{AFs}). One proposed method for deriving chemical-specific HK_{AFs} that account for inter-individual variability is to divide the 95th percentile for the sensitive subpopulation by the median value for the general healthy population (Lipscomb *et al.*, 2004). For all of the chemicals evaluated, the average estimated HK_{AFs} were greater than the default uncertainty factor of 3.2 with a range between 3.1- and 13.1-fold. Our results with these nine compounds suggest that the default value does not afford sufficient protection for sensitive populations, which for most of the chemicals was the pediatric life stage group (0–0.5 years). This is important in that initial studies that did not consider enzyme differences suggested that children would be adequately covered by the default uncertainty factor due to increased elimination or clearance of chemicals compared with adults (Renwick, 1998; Renwick and Lazarus, 1998). Separation of the variability associated with physiologic differences from differing enzyme rates in this study confirms the minor role physiology plays in this regard, supporting, to a degree, these earlier conclusions. Subsequent consideration of polymorphic metabolism or enzyme differences between healthy adults and neonates has led to the realization that the default uncertainty factor could be exceeded for certain chemicals (Dorne and Renwick, 2005; Ginsberg *et al.*, 2005, 2002, 2004; Hattis *et al.*, 2003). Although earlier papers relied on an overall understanding of differing enzyme abundances to draw these conclusions, the current work provides clearance information at the isozyme level and quantifies the impact of both enzyme differences and physiology on subpopulation variability. Although of moderate throughput, quantitation of chemical-specific HK_{AFs} in this manner could prove useful when applied more widely to the risk assessment process.

The second application was to estimate subpopulation-specific oral equivalent dose values associated with *in vitro* HTS assays to aid in chemical prioritization and identifying subpopulations with greater susceptibility to potential pathway perturbations. For most of the chemicals evaluated, the subpopulation-specific oral equivalent doses were significantly lower than the corresponding estimates of human exposure. Regulatory exposure estimates were not generated for carbaryl, the chemical with the largest HK_{AF}, as they were not deemed appropriate given the rapid recovery from carbaryl-induced acetylcholinesterase inhibition (USEPA, 2007). However, one chemical, fludioxonil, had oral equivalent dose values that overlapped exposure estimates for two pediatric subpopulations. This overlap indicates that the estimated exposures could lead to blood concentrations similar to those that elicited activity in the *in vitro* HTS assays. Although the comparison of subpopulation-specific oral equivalent dose values with corresponding exposure estimates can be useful for chemicals such as fludioxonil, the cost and analytical chemistry workload for generating the isozyme-specific clearance rates is significantly greater. In all the chemicals analyzed in this study, the maximum difference between the AERs for the healthy adult population and the most sensitive subpopulation was 7.1-fold. Given this difference, it makes sense to apply this approach only as a second tier screen where the margin of exposure between the oral equivalent dose values for the healthy adult population and the exposure estimate for the most highly exposed subpopulation is less than 100.

Apart from PK differences, pharmacodynamic variability will also need to be incorporated for ultimate application to risk assessment. The pharmacodynamic variability needs to address both genetic and age-related differences. High-throughput evaluation of population-based genetic differences in pharmacodynamic response was recently conducted using 81 lymphoblast cell lines derived from 27 mother-father-child trios (Lock *et al.*, 2012). The 81 lymphoblast cell lines were exposed to 240 chemicals in concentration-response format and differences in cytotoxicity and apoptosis were measured. The results showed chemical-specific variability between the cell lines for the endpoints assessed suggesting that the approach may be used as a surrogate measure of genetic variability across a population.

Age-related pharmacodynamic variability is a separate parameter that will be difficult to capture in either an HTS framework or using conventional tools. However, continued screening of chemicals across a broad range of molecular and pathway-based targets together with better characterization as to the ontological expression of these targets could be used to qualitatively identify age-related susceptibilities. In addition, combining the *in vitro* assay data with computational modeling will help to quantitatively evaluate the extent of the susceptibility when target pathways are known.

The development of new toxicity testing paradigms will rely heavily on *in vitro* HTS assays together with parallel investments in characterizing the pharmacokinetics and exposure levels of these chemicals. However, in order to translate the *in vitro* HTS results into risk assessment, PK and pharmacodynamic variability will need to be incorporated. A previous study outlining a framework for high-throughput risk assessment used simplifying default assumptions for the distribution of population-variability (Judson *et al.*, 2011). In this study, we present an experimental approach for estimating chemical-specific PK variability across multiple subpopulations. When integrated with promising approaches for estimating pharmacodynamic variability (Lock *et al.*, 2012) and subpopulation-specific exposure estimates, the combination provides a significant step toward enabling high-throughput chemical risk assessment.

SUPPLEMENTARY DATA

Supplementary data are available online at http://toxsci.oxfordjournals.org/.

FUNDING

American Chemistry Council's Long-Range Research Initiative; Agilent Thought Leader Award, Agilent Foundation.

ACKNOWLEDGMENTS

The authors thank David Billings, Alina Efremenko, Eric Healy, and Longlong Yang for their technical assistance, Masoud Jamei for his invaluable advice, and Simcyp Limited for providing access to Simcyp Simulator and Simcyp Pediatric under a not-for-profit license agreement. Lisa Almond is an employee of Simcyp Limited (a Certara company).

REFERENCES

Andersen, M. E. and Krewski, D. (2009). Toxicity testing in the 21st century: Bringing the vision to life. *Toxicol. Sci.* **107**, 324–330.

Besunder, J. B., Reed, M. D. and Blumer, J. L. (1988a). Principles of drug biodisposition in the neonate. A critical evaluation of the pharmacokinetic-pharmacodynamic interface (Part I). *Clin. Pharmacokinet.* **14**, 189–216.

Besunder, J. B., Reed, M. D. and Blumer, J. L. (1988b). Principles of drug biodisposition in the neonate. A critical evaluation of the pharmacokinetic-pharmacodynamic interface (Part II). *Clin. Pharmacokinet.* **14**, 261–286.

Blaauboer, B. J. (2010). Biokinetic modeling and in vitro-in vivo exptrapolations. *J. Toxicol. Environ. Health B* **13**, 242–252.

Bramer, S. L., Brisson, J., Corey, A. E. and Mallikaarjun, S. (1999). Effect of multiple cilostazol doses on single dose lovastatin pharmacokinetics in healthy volunteers. *Clin. Pharmacokinet.* **37(Suppl. 2)**, 69–77.

Chauret, N., Gauthier, A. and Nicoll-Griffith, D. A. (1998). Effect of common organic solvents on in vitro cytochrome P450-mediated metabolic activities in human liver microsomes. *Drug Metab. Dispos.* **26**, 1–4.

Cockcroft, D. W. and Gault, M. H. (1976). Prediction of creatinine clearance from serum creatinine. *Nephron* **16**, 31–41.

Cohen Hubal, E. A., Richard, A., Aylward, L., Edwards, S., Gallagher, J., Goldsmith, M. R., Isukapalli, S., Tornero-Velez, R., Weber, E. and Kavlock, R. (2010). Advancing exposure characterization for chemical evaluation and risk assessment. *J. Toxicol. Environ. Health B Crit. Rev.* **13**, 299–313.

Collins, F. S., Gray, G. M. and Bucher, J. R. (2008). Toxicology. Transforming environmental health protection. *Science* **319**, 906–907.

Cresteil, T. (1998). Onset of xenobiotic metabolism in children: Toxicological implications. *Food Addit. Contam.* **15**, 45–51.

Crewe, H. K., Barter, Z. E., Yeo, K. R. and Rostami-Hodjegan, A. (2011). Are there differences in the catalytic activity per unit enzyme of recombinantly expressed and human liver microsomal cytochrome P450 2C9? A systematic investigation into inter-system extrapolation factors. *Biopharm. Drug Dispos.* **32**, 303–318.

Croom, E. L., Stevens, J.C., Hines, R.N., Wallace, A.D. and Hodgson, E. (2009). Human Hepatic CYP2B6 developmental expression: The impact of age and genotype. *Biochem. Pharmacol.* **78**, 184–190.

Dickinson, G. L. and Rostami-Hodjegan, A. (2008). *Building virtual human populations: Assessing the propagation of genetic variability in drug metabolism to pharmacokinetics and pharmacodynamics*. In *Biosimulation in Drug Development* (M. Bertau, E. Mosekilde and H. V. Westerhoff Eds.), Wiley-VCH, Weinheim, Germany, pp.425–446.

Dix, D. J., Houck, K. A., Martin, M. T., Richard, A. M., Setzer, R. W. and Kavlock, R. J. (2007). The ToxCast program for prioritizing toxicity testing of environmental chemicals. *Toxicol. Sci.* **95**, 5–12.

Donato, M. T. and Castell, J. V. (2003). Strategies and molecular probes to investigate the role of cytochrome P450 in drug metabolism: Focus on in vitro studies. *Clin. Pharmacokinet.* **42**, 153–178.

Dorne, J. L. (2010). Metabolism, variability and risk assessment. *Toxicology* **268**, 156–164.

Dorne, J. L. and Renwick, A. G. (2005). The refinement of uncertainty/safety factors in risk assessment by the incorporation of data on toxicokinetic variability in humans. *Toxicol. Sci.* **86**, 20–26.

EPA (2003). *A Framework for a Computational Toxicology Research Program in ORD*. US Environmental Protection Agency, Washington, DC.

EPA (2005). *Guidelines for Carcinogen Risk Assessment*. US Environmental Protection Agency, Risk Assessment Forum, Washington, DC.

EPA (2011). Exposure Factors Handbook: 2011 Edition, EPA/600/R-09/052F. National Center for Environmental Assessment, Washington, DC.

Fisher, M. B., Paine, M. F., Strelevitz, T. J. and Wrighton, S. A. (2001). The role of hepatic and extrahepatic UDP-glucuronosyltransferases in human drug metabolism. *Drug Metab. Rev.* **33**, 273–297.

Gibson, C. R., Lu, P., Maciolek, C., Wudarski, C., Barter, Z., Rowland-Yeo, K., Stroh, M., Lai, E. and Nicoll-Griffith, D. A. (2013). Using human recombinant UDP-glucuronosyltransferase isoforms and a relative activity factor approach to model total body clearance of laropiprant (MK-0524) in humans. *Xenobiotica* **43**, 1027–1036.

Ginsberg, G., Slikker, W., Jr, Bruckner, J. and Sonawane, B. (2004). Incorporating children's toxicokinetics into a risk framework. *Environ. Health Perspect.* **112**, 272–283.

Ginsberg, G., Hattis, D., Russ, A. and Sonawane, B. (2005). Pharmacokinetic and pharmacodynamic factors that can affect sensitivity to neurotoxic sequelae in elderly individuals. *Environ. Health Perspect.* **113**, 1243–1249.

Ginsberg, G., Hattis, D., Sonawane, B., Russ, A., Banati, P., Kozlak, M., Smolenski, S. and Goble, R. (2002). Evaluation of child/adult pharmacokinetic differences from a database derived from the therapeutic drug literature. *Toxicol. Sci.* **66**, 185–200.

Gregory, P. A., Lewinsky, R. H., Gardner-Stephen, D. A. and Mackenzie, P. I. (2004). Regulation of UDP glucuronosyltransferases in the gastrointestinal tract. *Toxicol. Appl. Pharmacol.* **199**, 354–363.

Hallifax, D., Foster, J. A. and Houston, J. B. (2010). Prediction of human metabolic clearance from in vitro systems: Retrospective analysis and prospective view. *Pharm. Res.* **27**, 2150–2161.

Harper, T. W. and Brassil, P. J. (2008). Reaction phenotyping: Current industry efforts to identify enzymes responsible for metabolizing drug candidates. *AAPS J.* **10**, 200–207.

Hattis, D., Ginsberg, G., Sonawane, B., Smolenski, S., Russ, A., Kozlak, M. and Goble, R. (2003). Differences in pharmacokinetics between children and adults–II. Children's variability in drug elimination half-lives and in some parameters needed for physiologically-based pharmacokinetic modeling. *Risk Anal.* **23**, 117–142.

Hines, R. N. (2007). Ontogeny of human hepatic cytochromes P450. *J. Biochem. Mol. Toxicol.* **21**, 169–175.

Hiratsuka, M. (2012). In vitro assessment of the allelic variants of cytochrome P450. *Drug Metab. Pharmacokinet.* **27**, 68–84.

Hornung, R. W. and Reed, L. D.. (1990). Estimation of average concentration in the presence of nondetectable values. *Appl. Occup. Environ. Hyg.*, **5**, 46–51.

Houck, K. A., Dix, D. J., Judson, R. S., Kavlock, R. J., Yang, J. and Berg, E. L. (2009). Profiling bioactivity of the ToxCast chemical library using BioMAP primary human cell systems. *J. Biomol. Screen.* **14**, 1054–1066.

Howgate, E. M., Rowland Yeo, K., Proctor, N. J., Tucker, G. T. and Rostami-Hodjegan, A. (2006). Prediction of in vivo drug clearance from in vitro data. I: Impact of inter-individual variability. *Xenobiotica* **36**, 473–497.

Huang, R., Xia, M., Cho, M. H., Sakamuru, S., Shinn, P., Houck,

K. A., Dix, D. J., Judson, R. S., Witt, K. L., Kavlock, R. J., *et al.* (2011). Chemical genomics profiling of environmental chemical modulation of human nuclear receptors. *Environ. Health Perspect.* **119**, 1142–1148.

IPCS (2005). *Chemical-specific adjustment factors for interspecies differences and human variability: Guidance document for use of data in dose/concentration-response assessment*. Harmonization Project Document No. 2. World Health Organization, International Programme on Chemical Safety, Geneva, Switzerland.

Jamei, M., Marciniak, S., Feng, K., Barnett, A., Tucker, G. and Rostami-Hodjegan, A. (2009). The Simcyp((R)) population-based ADME simulator. Exp. Opin. Drug Metab. Toxicol., **5**, 211–223.

Jamroz, R. C., Guerrero, F. D., Pruett, J. H., Oehler, D. D. and Miller, R. J. (2000). Molecular and biochemical survey of acaricide resistance mechanisms in larvae from Mexican strains of the southern cattle tick, Boophilus microplus. *J. Insect Physiol.* **46**, 685–695.

Johnson, T. N., Rostami-Hodjegan, A. and Tucker, G. T. (2006). Prediction of the clearance of eleven drugs and associated variability in neonates, infants and children. *Clin. Pharmacokinet.* **45**, 931–956.

Johnsrud, E. K., Koukouritaki, S.B., Divakaran, K., Brunengraber, L.L., Hines, R.N. and McCarver, D.G. (2003). Human hepatic CYP2E1 expression during development. *J. Pharmacol. Exp. Ther.* **307**, 402–407.

Judson, R. S., Houck, K. A., Kavlock, R. J., Knudsen, T. B., Martin, M. T., Mortensen, H. M., Reif, D. M., Rotroff, D. M., Shah, I., Richard, A. M., *et al.* (2010). In vitro screening of environmental chemicals for targeted testing prioritization: the ToxCast project. *Environ. Health Perspect.* **118**, 485–492.

Judson, R. S., Kavlock, R. J., Setzer, R. W., Cohen Hubal, E. A., Martin, M. T., Knudsen, T. B., Houck, K. A., Thomas, R. S., Wetmore, B. A. and Dix, D. J. (2011). Estimating toxicity-related biological pathway altering doses for high-throughput chemical risk assessment. *Chem. Res. Toxicol.* **24**, 451–462.

Kavlock, R., Ankley, G. T., Collette, T., Francis, E., Hammerstrom, K., Fowle, J., Tilson, H., Toth, G., Schmieder, P., Veith, G. D., *et al.* (2005). Computational toxicology: Framework, partnerships, and program development. September 29–30, 2003, Research Triangle Park, North Carolina. *Reprod. Toxicol.* **19**, 265–280.

Kavlock, R. J., Austin, C. P. and Tice, R. R. (2009). Toxicity testing in the 21st century: Implications for human health risk assessment. *Risk Anal.* **29**, 485–487; discussion 492–497.

Kearns, G. L., Abdel-Rahman, S. M., Alander, S. W., Blowey, D. L., Leeder, J. S. and Kauffman, R. E. (2003). Developmental pharmacology–drug disposition, action, and therapy in infants and children. *N. Engl. J. Med.* **349**, 1157–1167.

King, C. D., Rios, G. R., Green, M. D. and Tephly, T. R. (2000). UDP-glucuronosyltransferases. *Curr. Drug Metab.* **1**, 143–161.

Knight, A. W., Little, S., Houck, K., Dix, D., Judson, R., Richard, A., McCarroll, N., Akerman, G., Yang, C., Birrell, L., *et al.* (2009). Evaluation of high-throughput genotoxicity assays used in profiling the US EPA ToxCast chemicals. *Regul. Toxicol. Pharmacol.* **55**, 188–199.

Knudsen, T. B., Houck, K. A., Sipes, N. S., Singh, A. V., Judson, R. S., Martin, M. T., Weissman, A., Kleinstreuer, N. C., Mortensen, H. M., Reif, D. M., *et al.* (2011). Activity profiles of 309 ToxCast chemicals evaluated across 292 biochemical targets. *Toxicology* **282**, 1–15.

Kothare, P. A., Linnebjerg, H., Skrivanek, Z., Reddy, S., Mace, K., Pena, A., Han, J., Fineman, M. and Mitchell, M. (2007). Exenatide effects on statin pharmacokinetics and lipid response. *Int. J. Clin. Pharmacol. Ther.* **45**, 114–120.

Koukouritaki, S. B., Manro, J.R., Marsh, S.A., Stevens, J.C., Rettie, A.E., McCarver, D.G. and Hines, R.N. (2004). Developmental expression of human hepatic CYP2C9 and CYP2C19. *J. Pharmacol. Exp. Ther.* **308**, 965–974.

Leakey, J. E., Hume, R. and Burchell, B. (1987). Development of multiple activities of UDP-glucuronyltransferase in human liver. *Biochem. J.* **243**, 859–861.

Lipscomb, J. C., Meek, M. E., Krishnan, K., Kedderis, G. L., Clewell, H. and Haber, L. (2004). Incorporation of pharmacokinetic and pharmacodynamic data into risk assessments. *Toxicol. Mech. Methods* **14**, 145–158.

Lipscomb, J. C. and Poet, T. S. (2008). In vitro measurements of metabolism for application in pharmacokinetic modeling. *Pharmacol. Ther.* **118**, 82–103.

Lock, E. F., Abdo, N., Huang, R., Xia, M., Kosyk, O., O'Shea, S. H., Zhou, Y. H., Sedykh, A., Tropsha, A., Austin, C. P., *et al.* (2012). Quantitative high-throughput screening for chemical toxicity in a population-based in vitro model. *Toxicol. Sci.* **126**, 578–588.

Martin, M. T., Dix, D. J., Judson, R. S., Kavlock, R. J., Reif, D. M., Richard, A. M., Rotroff, D. M., Romanov, S., Medvedev, A., Poltoratskaya, N., *et al.* (2010). Impact of environmental chemicals on key transcription regulators and correlation to toxicity end points within EPA's ToxCast program. *Chem. Res. Toxicol.* **23**, 578–590.

May, D. G., Naukam, R. J., Kambam, J. R. and Branch, R. A. (1992). Cimetidine-carbaryl interaction in humans: Evidence for an active metabolite of carbaryl. *J. Pharmacol. Exp. Ther.* **262**, 1057–1061.

McGraw, J. and Waller, D. (2012). Cytochrome P450 variations in different ethnic populations. *Expert Opin. Drug Metab. Toxicol.* **8**, 371–382.

Meek, M. E., Renwick, A., Ohanian, E., Dourson, M., Lake, B., Naumann, B. D. and Vu, V. (2002). Guidelines for application of chemical-specific adjustment factors in dose/concentration-response assessment. *Toxicology* **181–182**, 115–120.

Mignini, F., Tomassoni, D., Streccioni, V., Traini, E. and Amenta, F. (2008). Pharmacokinetics and bioequivalence study of two tablet formulations of lovastatin in healthy volunteers. *Clin. Exp. Hypertens.* **30**, 95–108.

Mihara, K., Suzuki, A., Kondo, T., Yasui, N., Furukori, H., Nagashima, U., Otani, K., Kaneko, S. and Inoue, Y. (1999). Effects of the CYP2D6*10 allele on the steady-state plasma concentrations of haloperidol and reduced haloperidol in Japanese patients with schizophrenia. *Clin. Pharmacol. Ther.* **65**, 291–294.

Miyagi, S. J. and Collier, A. C. (2007). Pediatric development of glucuronidation: The ontogeny of hepatic UGT1A4. *Drug Metab. Dispos.* **35**, 1587–1592.

NRC (1983). *Risk Assessment in the Federal Government: Managing the Process*. National Academy Press, Washington, DC.

NRC (1993). *Pesticides in the Diets of Infants and Children*. National Research Council of the National Academies, Washington, DC.

NRC (2007). *Toxicity Testing in the 21st Century: A Vision and a Strategy*. National Academy Press, Washington, DC.

NRC (2009). *Science and Decisions: Advancing Risk Assessment*. National Academies Press. Washington, DC.

Pinto, N. and Dolan, M. E. (2011). Clinically relevant genetic variations in drug metabolizing enzymes. *Curr. Drug Metab.* **12**, 487–497.

Proctor, N. J., Tucker, G. T. and Rostami-Hodjegan, A. (2004). Predicting drug clearance from recombinantly expressed CYPs:

Intersystem extrapolation factors. *Xenobiotica* **34**, 151–178.
Renwick, A. G. (1998). Toxicokinetics in infants and children in relation to the ADI and TDI. *Food Addit. Contam.* **15(Suppl. 1)**, 17–35.
Renwick, A. G. and Lazarus, N. R. (1998). Human variability and noncancer risk assessment–an analysis of the default uncertainty factor. *Regul. Toxicol. Pharmacol.* **27**, 3–20.
Ritter, J. K. (2007). Intestinal UGTs as potential modifiers of pharmacokinetics and biological responses to drugs and xenobiotics. *Expert Opin. Drug Metab. Toxicol.* **3**, 93–107.
Rotroff, D. M., Beam, A. L., Dix, D. J., Farmer, A., Freeman, K. M., Houck, K. A., Judson, R. S., LeCluyse, E. L., Martin, M. T., Reif, D. M., *et al.* (2010a). Xenobiotic-metabolizing enzyme and transporter gene expression in primary cultures of human hepatocytes modulated by ToxCast chemicals. *J. Toxicol. Environ. Health B Crit. Rev.* **13**, 329–346.
Rotroff, D. M., Wetmore, B. A., Dix, D. J., Ferguson, S. S., Clewell, H. J., Houck, K. A., Lecluyse, E. L., Andersen, M. E., Judson, R. S., Smith, C. M., *et al.* (2010b). Incorporating human dosimetry and exposure into high-throughput in vitro toxicity screening. *Toxicol. Sci.* **117**, 348–358.
Rowland-Yeo, K., Rostami-Hodjegan, A. and Tucker, G.T. (2003). Abundance of cytochrome P450 in human liver: A meta analysis. *Br. J. Clin. Pharmacol.* **57**, 687–688.
Rubin, M., Bruck, E and Rapoport, M (1949). Maturation of renal function in childhood: Clearance studies. *J. Clin. Invest.* **28**, 1144–1162.
Salem, F., Rostami-Hodjegan, A. and Johnson, T. N. (2013). Do children have the same vulnerability to metabolic drug-drug interactions as adults? A critical analysis of the literature. *J. Clin. Pharmacol.* **53**, 559–566.
Schmucker, D. L. (2005). Age-related changes in liver structure and function: Implications for disease ? *Exp. Gerontol.* **40**, 650–659.
Singh, D., Kashyap, A., Pandey, R. V. and Saini, K. S. (2011). Novel advances in cytochrome P450 research. *Drug Discov. Today* **16**, 793–799.
Stringer, R. A., Strain-Damerell, C., Nicklin, P. and Houston, J. B. (2009). Evaluation of recombinant cytochrome P450 enzymes as an in vitro system for metabolic clearance predictions. *Drug Metab. Dispos.* **37**, 1025–1034.
Suzuki, A., Yasui-Furukori, N., Mihara, K., Kondo, T., Furukori, H., Inoue, Y., Kaneko, S. and Otani, K. (2003). Histamine H1-receptor antagonists, promethazine and homochlorcyclizine, increase the steady-state plasma concentrations of haloperidol and reduced haloperidol. *Ther. Drug Monit.* **25**, 192–196.
Tanaka, E. (1998). In vivo age-related changes in hepatic drug-oxidizing capacity in humans. *J. Clin. Pharm. Ther.* **23**, 247–255.
Tan, Y. M., Liao, K. H. and Clewell, H. J., 3rd (2007). Reverse dosimetry: Interpreting trihalomethanes biomonitoring data using physiologically based pharmacokinetic modeling. *J. Expo. Sci. Environ. Epidemiol.* **17**, 591–603.
Thelen, K. and Dressman, J. B. (2009). Cytochrome P450-mediated metabolism in the human gut wall. *J. Pharm. Pharmacol.* **61**, 541–558.
Tukey, J. W. (1977). *Exploratory Data Analysis*. Addison-Wesley. ReadingMA.
Tukey, R. H. and Strassburg, C. P. (2000). Human UDP-glucuronosyltransferases: Metabolism, expression, and disease. *Annu. Rev. Pharmacol. Toxicol.* **40**, 581–616.
USEPA (2007). *Reregistration Eligibility Decision for Carbaryl*. US Environmental Protection Agency, Washington, DC.
Venkatakrishnan, K., von Moltke, L. L., Court, M. H., Harmatz, J. S., Crespi, C. L. and Greenblatt, D. J. (2000). Comparison between cytochrome P450 (CYP) content and relative activity approaches to scaling from cDNA-expressed CYPs to human liver microsomes: Ratios of accessory proteins as sources of discrepancies between the approaches. *Drug Metab. Dispos.* **28**, 1493–1504.
Wetmore, B. A. (2014). Quantitative in vitro-to-in vivo extrapolation in a high-throughput environment. Toxicology doi: 10.1016/j.tox.2014.05.012. [Epub ahead of print]
Wetmore, B. A., Wambaugh, J. F., Ferguson, S. S., Sochaski, M. A., Rotroff, D. M., Freeman, K., Clewell, H. J., III, Dix, D. J., Andersen, M. E., Houck, K. A., *et al.* (2012). Integration of dosimetry, exposure, and high-throughput screening data in chemical toxicity assessment. *Toxicol. Sci.* **125**, 157–174.
Whyard, S., Russell, R. J. and Walker, V. K. (1994). Insecticide resistance and malathion carboxylesterase in the sheep blowfly, Lucilia cuprina. *Biochem. Genet.* **32**, 9–24.
Yasui-Furukori, N., Kondo, T., Mihara, K., Suzuki, A., Inoue, Y., De Vries, R. and Kaneko, S. (2002). Lack of correlation between the steady-state plasma concentrations of haloperidol and risperidone. *J. Clin. Pharmacol.* **42**, 1083–1088.
Yokoi, T. (2009). Essentials for starting a pediatric clinical study (1): Pharmacokinetics in children. *J. Toxicol. Sci.* **34(Suppl. 2)**, SP307–SP312.